ROYAL SOCIETY OF CHEMISTRY

Analyst

Characterising cytotoxic agent action as a function of the cell cycle using Fourier Transform Infrared Mircospectroscopy

SCHOLARONE™
Manuscripts

Characterising cytotoxic agent action as a function of the cell cycle using Fourier Transform Infrared Mircospectroscopy

M. Jimenez-Hernandez [a,b], M.D. Brown [b], C. Hughes [a,b], N.W Clarke [b,c,d] and P. Gardner [a*].

[a]Manchester Institute of Biotechnology, University of Manchester, 131 Princess Street, Manchester, UK M1 7DN.

[b]Genito-Urinary Cancer Research Group, Institute for Cancer Sciences, Paterson Building, University of Manchester, The Christie NHS Foundation Trust, Manchester Academic Health Sciences Centre, Manchester, UK M20 4BX

[c]Department of Urology, The Christie NHS Foundation Trust, Manchester, UK, M20 4BX, UK

[d]Department of Urology, Salford Royal Hospital NHS Foundation Trust, Stott Lane, Salford, M6 8HD

* Corresponding author: e-mail: peter.gardner@manchester.ac.uk

Abstract

Fourier Transform Infrared (FTIR) micro-spectroscopy measurements were acquired to study infrared signatures of chemotherapeutic response as a function of the cell cycle. Renal carcinoma Caki-2 cells were exposed to IC_{50} doses of 5-Fluorouracil and Paclitaxel for a period of 24 hours. The inherent cell cycle infrared signatures from untreated and drug-treated cells were successfully retrieved by the construction of a robust SVM able to discriminate the cell cycle phases of this cell line with an average accuracy of 83.7%. The overriding infrared signature observed relates to an apoptotic biochemical response that does not appear to be correlated with the events affected by the drugs' mode of action or the cell cycle. Since apoptosis is a well conserved mechanism among living species, these results suggest that both the stages of proliferation as well as the absence/presence of apoptosis need to be taken into account in order to elucidate the fine biochemical details revealing the immediate cellular response to the drug in order to assign reliable spectral patterns of drug action.

Introduction

Chemotherapy, along with surgery and radiotherapy, remains as one of the main approaches for treating cancer. The principle is to preferentially kill or prevent the proliferation of neoplastic cells due to their relatively higher duplication rate, compared with healthy cells. Ideally, any anticancer agent used for treating a cancer patient should selectively destroy cancer cells. However, healthy cells are also exposed to cytotoxic agents, leading to side effects such as gastrointestinal tract lesions and bone marrow suppression (*1-2*).

While it is true that the nature of the tumour has an important role in the overall treatment/outcome of the patient, (*e.g.* renal cancers are known to be inherently more resistant to chemotherapy than their prostate counterparts) it is also important to point out that the current philosophy of chemotherapy is still very "broad" since it aims to kill as many cells as possible by exposing the cancer patient to a "maximum tolerated dose" followed by several rest cycles that ultimately lead to the cyclic growth of the tumour and concomitant enrichment of a population with a more aggressive cellular phenotype.

Recently, a new approach termed "metronomic chemotherapy" has arisen in order to treat cancer as a chronic disease in which treatment would be delivered for a longer period of time at a lower dose and with shorter resting cycles (*3*).

However the key issue of patient management for chemotherapeutic treatment selection and monitoring therapeutic response still remains. Consequently, the need for reliable methods to evaluate early response to the action of chemotherapy drugs is of utmost importance.

In recent years, FTIR micro-spectroscopy has proved to be a cost-effective, non-destructive and reliable technique able to interrogate biological specimens. In particular it has been used in order to highlight the biochemical features of cancerous cells exposed to several drugs and which modes of

1
2
3
4
5
6
7
8
9
10
11
12
13
14
15
16
17
18
19
20
21
22
23
24
25
26
27
28
29
30
31
32
33
34
35
36
37
38
39
40
41
42
43
44
45
46
47
48
49
50
51
52
53
54
55
56
57
58
59
60

action were known to be different: anti-metabolites, DNA interactive agents, anti-tubulin agents, cardiotonic steroids, platinum and gold derivatives and Tyrosine Kinase Inhibitors(*4-20*).

In this study, the FTIR spectral profiles of Caki-2 cells exposed to either paclitaxel or 5FU have been analysed as a function of the cell cycle in order to determine whether the differential response induced by these two drugs, known to act via distinct modes of action, could be revealed by means of FTIR spectroscopy. Although Derenne *et al.(17)* have recently shown that the influence of the cell cycle is "small" compared with the overall effect of paclitaxel on PC-3 cells cultured *in-vitro*, our study aimed to (a) demonstrate the capability of FTIR spectroscopy for retrieving the cell cycle phase of untreated and drug-treated cells via the construction of a robust SVM, (b) highlight the metabolic modifications induced by the drugs also in the S-phase of development and (c) exploit the potential of FTIR spectroscopy for providing supporting information regarding the cell cycle phases of development of Caki-2 in order to identify fine biochemical signatures due to different stimuli.

Paclitaxel and 5FU have been chosen on the basis on their known mode of action affecting particular events of the cell cycle. The incorporation of 5FU into the cells is followed by its intracellular conversion into active metabolites capable of acting as pyrimidine analogues that can be mis-incorporated into both RNA and DNA leading to lethal damage. Secondary cellular damage can be induced by the irreversible inhibition of the thymidylate synthetase, an enzyme that catalyses the conversion of deoxyuridine monophosphate (dUMP) to deoxythymidine monophosphate (dTMP). This therefore enriches the cellular culture in the S-phase of the cell cycle and ultimately leads to cellular death via a thymidine less pathway(*21*). Paclitaxel on the other hand exerts its action on G_2M stage of the cell cycle by stabilizing the microtubules, via a covalent bond with tubulin, and preventing cellular division(*22*).

Materials and Methods

Cell culture

Cells from the adherent clear cell renal carcinoma cell line Caki-2 were seeded in 3.8 cm^2 well plates (BD Falcon) at a concentration of 9000 cells/cm^2 in 1.5 mL of Dulbecco's modified Eagle's Medium (DMEM) (Sigma) supplemented with 1% L-glutamine and 15% of foetal calf serum (FCS) (Sigma). The wells were kept in a humidified atmosphere containing 5% CO_2 at 37 ^{o}C for 24 hours in order to allow attachment of the cells to the growth surface. After this initial seeding period, the cells were exposed for 24 hours at the IC_{50} concentration of 5FU or Paclitaxel obtained by means of the SRB assay method(*23*), 2.4 μM and 0.01 μM respectively. Untreated control cells were grown in parallel and each condition was replicated three times.

5-ethynyl-2'-deoxyuridine labelling (EdU).

After drug treatment, the cultures of Caki-2 cells were exposed to 10 μM of EdU (Life Technologies) for 1 hour in order to promote the incorporation of this nucleoside analogue of thymidine into the nascent DNA of S-phase cells.

FTIR sample preparation

Each well was washed with PBS (3 × 1 mL) followed by incubation with 400 μL of trypsin at 37 ^{o}C for 3 minutes. Detached cells were collected in 1 mL of DMEM supplemented with 1% L-glutamine and 15% FCS and the tubes were centrifuged for 5 minutes at 400g. The supernatant was discarded and the cellular pellet washed with PBS (2 × 1 mL) followed by formalin fixation for 30 minutes at room temperature(*24*). Fixed cells were washed with Hank's balanced salt solution (HBSS) (6 × 1 mL) and then spin deposited onto calcium fluoride (CaF$_2$) slides. The samples were washed with double distilled water (×3) and air dried for 24 hours prior FTIR data collection. Cells from the three independent culture replicates were then measured by FTIR randomly, over a period of three weeks, in order to eliminate any potential bias associated with time/day of measurement.

Focal Plane Array (FPA) imaging FTIR spectroscopy

The FTIR spectral mosaics were collected in transmission mode using a Varian (Agilent) 670 spectrometer with a 128 × 128 pixel Focal Plane Array (FPA), Mercury Cadmium Telluride (MCT) detector coupled with a Varian (Agilent) 620-IR microscope and a 15× Cassegrain objective. All the images were recorded by co-adding 128 or 256 interferograms per pixel for the sample and the background respectively with a spectral resolution of 4 cm^{-1}. A Blackmann-Harris apodisation function was used during processing, after which the 900 − 4000 cm^{-1} wavenumber range was retained with a final data spacing of 2 cm^{-1}. The same parameters were used to record the reference Matrigel spectrum (used in the data preprocessing stage) but in this case a single point MCT detector was used. Each spectral mosaic encompassed 9 individual tiles and therefore the collection time scaled up to 3.5 hours per image. The CaF$_2$ slides containing the FTIR-sampled cells were stained against cell cycle markers. After staining, the fluorescent data was visually inspected in order to create the pool of spectral data classified as a function of the cell cycle.

Data pre-processing

The FTIR spectral mosaics were subject to a written in-house algorithm (Matlab, Mathworks Inc.) in order to extract and reconstruct the individual spectrum per cell (*25-26*). Briefly, this algorithm creates a binary mask based on the quality test of the FTIR mosaic as a function of protein content; hence, the "blank" areas that do not correlate to a cell within the slide are not processed further. After removing the "blank" areas, each mosaic yielded an average of 320 cellular spectra; yet, visual inspection of each useful region in the image revealed that only a few spectra belonged to single isolated cells (as opposed to clumps of cells that also formed due to the deposition of cells onto the slide); hence the need for collecting multiple mosaics per condition. Clumps of cells were not included in this study at all as they may have included cells undergoing different cell cycle phases. The raw FTIR spectra were corrected for the effects of Resonant Mie Scattering (*27-28*) using the RMieS-EMSC algorithm and a Matrigel spectrum as reference and 100 iterations. Spectra before and

after the application of the RMieS-EMSC correction can be found in the supplementary information.

A total of 765 individual spectra were employed for data analysis and modelling.

Retrospective immunofluorescent staining of the samples

Identification of S-phase cells, EdU detection

The samples were rehydrated with 300 μL of PBS for 30 minutes at room temperature followed by permeabilisation via the addition of PBS containing 0.25% Triton X-100. After 15 minutes, the samples were washed with PBST (3×). EdU detection was performed by the addition of a PBS based solution containing 9.6 μL CuSO$_4$ and 1 μL Alexa fluor 647 (Life Technologies). The slides were incubated for 30 minutes at 25 ^{o}C and protected from light; the reaction was stopped by removing this solution and washing the slides with 100 μL of PBS (2 × 0.5 mL).

Cdt1 and Geminin detection for G$_1$ and G$_2$ phase cells respectively.

Identification of these two cell cycle markers was possible due to the utilization of the following primary antibodies: rabbit polyclonal anti-cdt1, mouse monoclonal rhodamine conjugated anti-geminin antibody and a fluorescein isothiocyanate (FITC) goat polyclonal pre-adsorbed anti-rabbit secondary antibody (Abcam). The primary antibodies were diluted at a final concentration of 12 μg/mL and 20 μg/mL respectively in 1% BSA/PBST. The secondary antibody was diluted at 7 μg/mL in 1% BSA/PBST.

After EdU incubation the slides were blocked with 1% BSA in PBST for 1 hour at room temperature and protected from light. After this time, the blocking solution was discarded followed by the addition of 200 μL of the solution containing the cocktail of primary antibodies and incubated for 2 hours at room temperature in dark.

The slides were washed with PBST (3×) followed by the addition of 200 μL of the pre-adsorbed anti-rabbit secondary antibody and incubated for 1 hour at room temperature protected from light. 3

PBST washes were performed followed by counterstaining with 2 μL of mounting media with DAPI (Life Technologies) and sealed with a 22 × 22 mm coverslip. The slides were dried overnight before collecting the fluorescent images.

Identification of the activated form of Caspase-3

The immunofluorescent detection of activated caspase-3 was conducted on different slides from those subjected to the retrospective staining for cell-cycle phase identification due to the complex antibody system used in this late procedure. The samples were rehydrated, permeabilised and blocked as before followed by the addition of 200 μL of a PBST based solution containing 3.5 μg/mL of anti-activated Caspase-3 DyLight-488 conjugated antibody (Abcam). The samples were incubated overnight at 4 °C. The slides were carefully washed with PBST (3×) and 2 μL of mounting media containing DAPI was used in order to counterstain the DNA and coverslip the slides.

The fluorescent images were collected using a Nikon Eclipse 90i microscope equipped with a super high-pressure mercury lamp and a D-FL Epi-Fluorescence attachment. The excitation wavelengths for the identification of DAPI, cdt1-FITC, geminin-TRITC and Edu-HcRed were 358, 494, 544 and 653 nm and the corresponding filters were blue, green, yellow and far-red respectively. The images were collected via a monochromatic DS-Qi1 camera.

Results and Discussion

Cell cycle phase assignment.

The unambiguous assignment of the cell cycle phase of each sampled cell was performed using immunofluorescent staining; thus, each FTIR spectrum was individually allocated within the pool of

data (G_0-G_1, S or G_2-M phase) that it belonged depending upon the staining pattern revealed by the retrospective staining (see Figure 1). After this qualitative cell cycle phase assignment, the spectral data from drug-treated cells was used as a blind test for previously constructed and reported linear SVM (*26*), as these models showed an overall good prediction accuracy when validated with FTIR data of untreated Caki-2 cells. When the SVM were tested with the drug-treated spectra, already classified as G_1, S or G_2-M phases by means of the IF staining, the performance of such models decreased by an average of 23%. Despite the fact that the cells were undergoing well-defined biochemical stages of proliferation; it is likely that the inherent cell-cycle dependent spectral features were masked by the pronounced biochemical features due to the cascade of events triggered by the anticancer drugs.

In isolation, this observation supports the fact that the cell cycle is not the main classification trend of drug-treated cellular spectra, as reported recently by Derenne *et al.*(*17*). An exhaustive analysis on the second derivative spectra of control (untreated spectra) and drug treated cells as a function of the cell cycle in G_1, S and G_2-M phases for both 5FU and paclitaxel, however, has revealed that it is too early to completely rule out the influence of the cell cycle in order to highlight different modes of action by means of FTIR spectroscopy and thus: differential response to treatment.
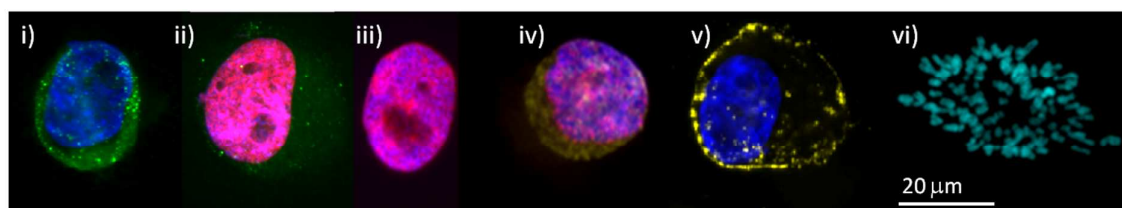
Figure 1. Composite fluorescent images of an asynchronous culture of Caki-2 cells on a CaF_2 slide collected under a 40× magnification lens for DAPI (blue), cdt1-FITC (green), geminin-TRITC (yellow) and EdU-HcRed (red) respectively. The label at the top identifies each cell with a particular cell cycle event: (i) G_1 phase, (ii) G_1-S phase transition, (iii) fully engaged S phase, (iv) S-G_2 phase transition, (v) fully engaged G_2 phase & (vi) mitosis (this image has been falsely coloured cyan in order to enhance the contrast between the DNA and the background). The integration time for image collection was 100 ms, 1 s, 1.5 s and 600 ms for blue, green, yellow and red respectively.

Spectral fingerprint of 5FU and paclitaxel treated Caki-2 cells as a function of the cell cycle.

Once classified as a function of the cell cycle by means of the IF staining protocol reported earlier(26), the pool of data encompassing both control and drug treated spectra were subjected to the computation of the second derivative with a smoothing window of 11 points via the Savitzky-Golay method(29) followed by vector normalisation in order to highlight the fine spectral features that otherwise would not be noticeable(30). Figure 2 shows the stacked plot of the second derivative spectra of drug-treated and untreated (control) cells as a function of the cell cycle divided into 5 spectral regions for clarity. Upon initial observation, the main spectral differences are observed between the spectra of control cells and those cells that were treated with a cytotoxic compound. In the high frequency spectral region (Figure 2 a), dominated by the stretching modes of methyl and methylene groups, 5FU and Paclitaxel are practically indistinguishable, displaying almost perfect superposition of the second derivatives for all respective cell cycle phases. Although the cytotoxic compounds used to treat Caki-2 cells in this study are known to act via two different modes of action, the spectral profiles indicate that there is a consistent change in the nature of the lipids leading to longer chains –hence the increase of the methylene groups respect to the methyl moieties– that does not seem to be dependent upon the action of any particular drug. Instead, it seems to be related to the cascade of events induced within the cells once exposed to a cytotoxic environment that is no longer optimal for normal growth. Such change in the lipids is shown in Figure 2 a) in the peaks at 2922 cm^{-1} and 2852 cm^{-1} corresponding to the asymmetric and symmetric stretch of the CH_2 contained in the acyl chain of lipids respectively(31).

In the region of the spectra from 1800 cm^{-1} to 1560 cm^{-1} (Figure 2 b), dominated by the carbonyl stretching mode of lipids, phospholipids and proteins(31), the main differences are observed between the control and the drug-treated spectra. Nevertheless, the drug-treated spectra belonging to both G_1 and S phase cells exhibit a more pronounced feature at 1741 cm^{-1} compared to G_2M-phase cells. Moreover, drug-treated G_2M-phase cells exhibit a relative decrease of the shoulder at 1711 cm^{-1}, when compared with the control. In all the cell cycle phases, there is a relative decrease of

intensity in the Amide I region, particularly in the peaks at 1679 cm^{-1} and 1657 cm^{-1} that are both

related to the vibration of the carbonyl group engaged in the protein linkage.

Altogether, these observations indicate that while there is an increase of carbonyl-based

biochemical compounds (such as lipids and phospholipids) within the cells (detected not only at

1741 cm^{-1} but also in the high frequency region of the spectra (Figure 2 a)), the overall content of

protein among all the cell cycle phases is decreasing with respect to control cells, irrespective of the

cytotoxic compound used to treat the cellular cultures of Caki-2 cells.

The reduction of protein content along with the change in the chain-length of the lipids within the

drug-treated cycling cells is also visualized in the Amide II region, from 1480 to 1575 cm^{-1}, and in the

CH_2 scissoring mode of the acyl chain in lipids at 1465 cm^{-1} respectively (see Figure 2 c). It is,

however, particularly evident in the Amide II region that such changes appear to be linked to both

the actual mode of action of the cytotoxic drugs and the cell cycle phase of the cells.

The peaks arising at 1517 cm^{-1}, 1532 cm^{-1} and 1547 cm^{-1}, largely due to the C-N stretching and in-

plane bending of the N-H group of proteins[32], show that such reduction of protein content is more

dramatic in spectra belonging to G_2M phase than in S phase cells or even G_1 phase cells compared

with their control counterparts.

Interestingly, S-phase spectra revealed cells to be more affected by 5FU drug treatment than cells

treated with paclitaxel, as the later display slightly more similar features to the control spectra of

"clean" S-phase cells, particularly in the reduced protein content displayed at 1547 cm^{-1}.

Figure 2 (d) shows that while S and G_2M drug-treated Caki-2 cells display a more resolved peak at

1402 cm^{-1} corresponding to the symmetric bending mode of the CH_3 group, the overall content of

phosphate-based compounds seems to be decreasing among all the cell cycle phases, compared

with the controls, as indicated by the peak at 1238 cm^{-1}. This observation is consistent with the

noticeably reduced infrared absorption of drug-treated cells displayed in the low frequency end of

the spectra (see Figure 2 e) at 1120 cm^{-1}and 1084 cm^{-1} corresponding to the symmetric

phophodiester stretching band of nucleic acids.

Finally, the low frequency end of the spectra (Figure 2 e) reflects the relative decrease of protein

content at 1172 cm^{-1} mainly in S and G$_2$M phase for both cytotoxic treatments, which is due to the

stretching modes of the C-OH groups of serine, threonine, and tyrosine residues of cellular

proteins(*31*). Furthermore, the peaks at 1152 cm^{-1} and 1105 cm^{-1}, (due to the absorbance of C-O

and C-C stretching and C-O-H deformation motions of carbohydrates in cells in the form of glycogen,

glycoproteins or sugars), slightly resolves those cells that have been treated with paclitaxel or 5FU.

Such absorption is, however, greater in spectra belonging to those cells that have been treated with

paclitaxel as displayed across all the cell cycle phases. The increased content of carbohydrates is also

revealed by the peaks at 1036 cm^{-1}and 1020 cm^{-1} due to the C-O stretch of carbohydrates

convoluted with skeletal *trans* conformation (C-C) of DNA.
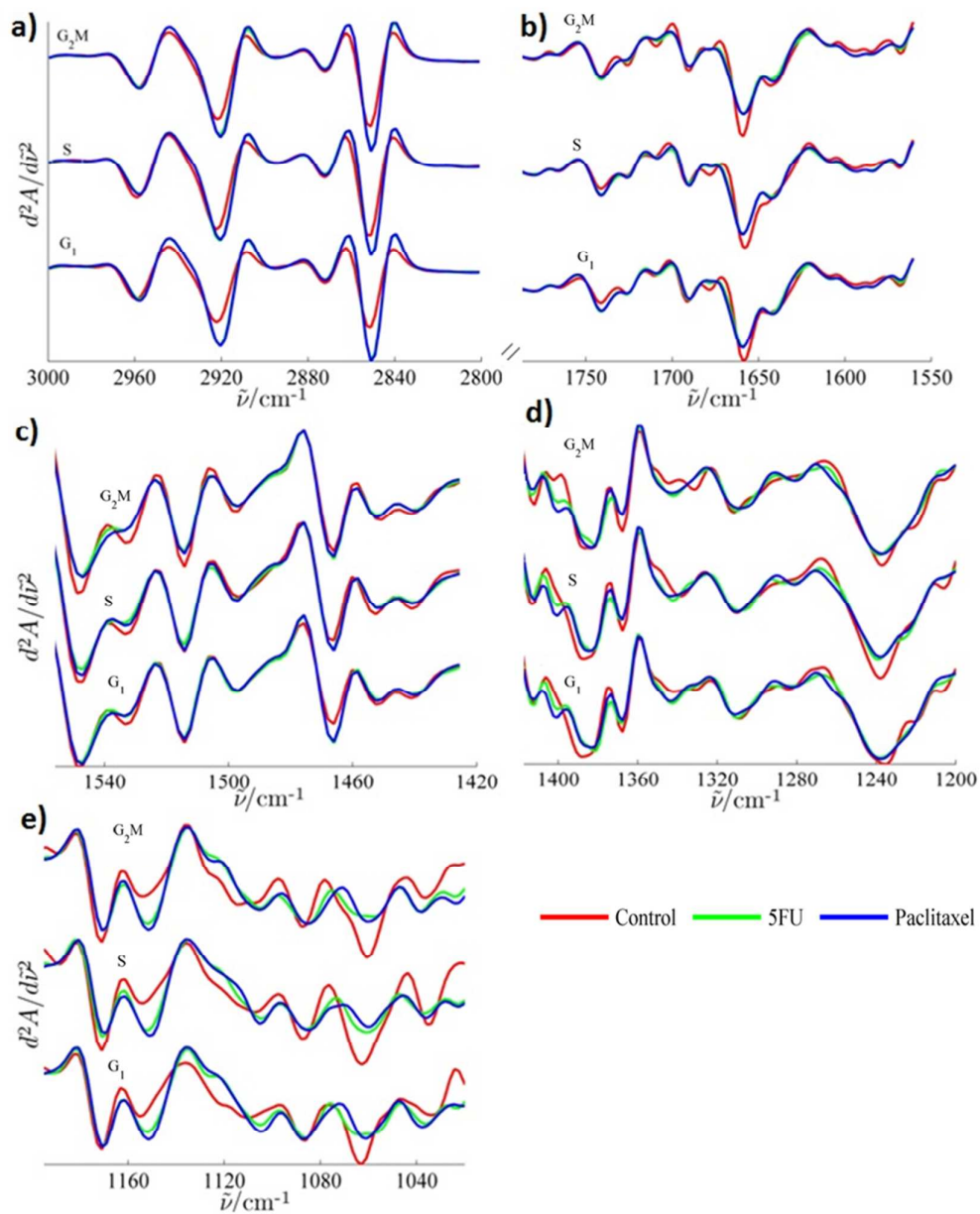
Figure 2. Stacked plot of the second derivative spectra of Control (red) and cells treated with 5FU (green) and Paclitaxel (blue) as a function of the cell cycle.

By analysing the infrared regions in Figure 2, it has been possible to identify that Caki-2 cells have a very similar biochemical response to two chemotherapeutic agents with different well defined modes of action. This cascade of events seems to be directing an overall trend in which the main features are both changes in the nature of the lipids and reduction of protein content among all cell

cycle phases, relative to their corresponding controls. These observations correlate with the spectroscopic features that have been historically reported for both inhibition of cellular growth([8]) and apoptosis, previously studied via the analysis of the FTIR spectra on cell-based models([33-34]) in animal and plant-based experiments investigated by means of Proton Magnetic Resonance Spectroscopy([35-36]). In 2009, Gasper *et al.*([9]) suggested that such modifications in the cellular lipidome may be reflecting the particular mode of action of PC-3 cells exposed to oubain; yet, the analysis of the lipid region against pure spectra of lipids revealed a strong contribution of peaks associated to phosphatidylserine. Interestingly, one of the biochemical hallmarks of apoptosis is the externalization of normal-inward facing residues of phosphatidylserine on the outer layers of the cellular membrane in order to facilitate the digestion of the cell via phagocytosis([37]). Conversely, Derenne *et al.*([4-5]) have recently shown that the mode of action of a particular drug is the leading clustering trend of drug-treated cells; however, the high-frequency region of the spectra (2800 cm^{-1} to 3000 cm^{-1}) describing the lipid content in the cells was excluded from the analysis as well as the potential physical distortions that may only be due to the cell cycle phase([26]) accumulation induced by the treatment with the drugs. In their following study([17]), these sources of variability were taken into consideration and, although only G_0-G_1 and G_2-M phases of the cell cycle exposed to 1 anticancer drug were involved in the analysis, the authors concluded that the inherent biochemical changes due to the cell cycle accounted for very little variation in the FTIR spectra of paclitaxel-treated cells. Interestingly, in this later publication by Derenne *et al.*([17]), the different spectra of drug-treated G_2-M phase cells against their untreated counterparts revealed that the "mode of action" of paclitaxel induced (a) an increased methylene signal from the lipids and (b) a reduction in the protein content: features that have been shown to be characteristic of cells undergoing an apoptotic response. It is therefore likely that the reduction in the protein content may be related to the degradation of cytoskeletal and nuclear proteins occurring soon after the apoptotic machinery is induced either by internal or external stimuli([37]). We observed similar spectral features within our treated paclitaxel cells (Figure 2) and more importantly in cells that have been treated with 5FU, and

therefore subjected to a completely different mode of drug action. In this regard, the following questions arise: is it possible that, in addition to the cell cycle dependency and the mode of action of the drugs, the FTIR spectral information is convoluted with a differential stage of apoptotic response?

In order to answer these questions it is necessary to interrogate both control and drug-treated samples against a reliable marker of apoptosis. Detection of activated caspase-3 is a standard method for determining whether a sample is undergoing apoptosis at the point of fixation or not(*37*). Caspase-3 is a proteolytic enzyme that exists in the cells as an inactive moiety but has the potential to amplify the apoptotic signals after being activated by a stimulus. Thus, if a given cell displays a positive staining for activated caspase-3 then that cell has started the apoptotic machinery that will ultimately lead to cell death. Figure 3 demonstrates that, after 24 hours, Caki-2 cells treated with the IC50 concentration of both 5FU and paclitaxel have initiated an apoptotic response due to the exposure to these two different drugs. Consequently, the FTIR spectra collected from these cellular cultures contain the biochemical features that are known to be related to apoptosis and the cell cycle phase inherent to each sampled cell.
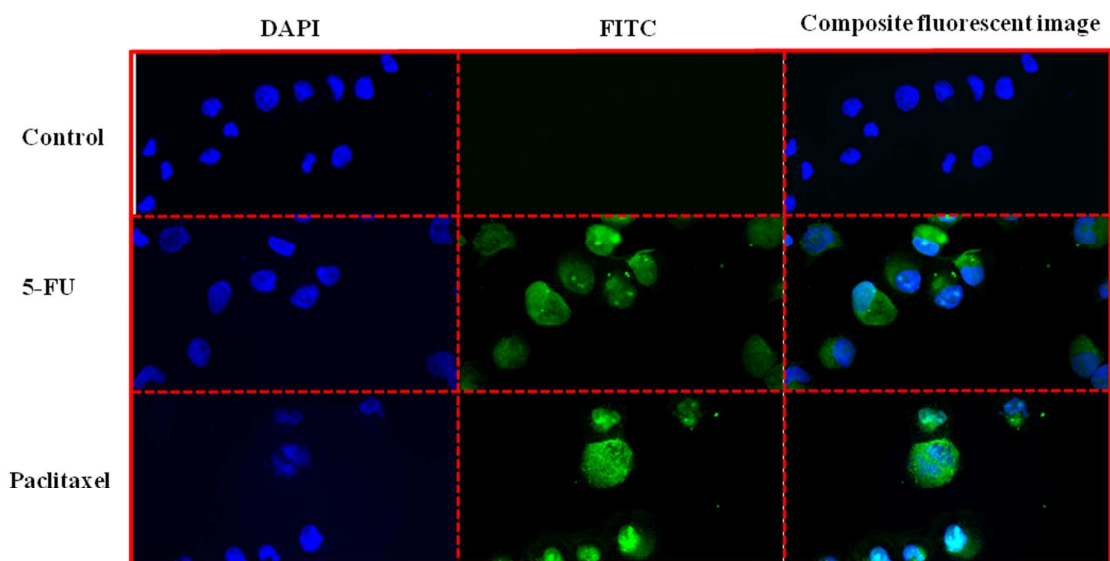
Figure 3. Detection of apoptosis: Caki-2 cells, untreated (control) and drug-treated (5FU and paclitaxel), stained for activated caspase-3 and counterstained with DAPI for DNA. The first column corresponds to the images collected under a

blue filter in order to collect the light emitted by the DAPI-stained nuclei of cells. The middle column displays images from the same field of view under a secondary green filter that enabled the visualisation of the light emitted by the DyLight- 488 conjugated Anti – Activated Caspase-3 antibody. The 3rd column is the composite image from both DAPI and FITC filters that gives place to the accurate identification of Caspase-3 within the cells.

Cell cycle dependent features, a PLSR approach.

The RMieS-EMSC corrected FTIR spectra was subjected to the multivariate analytical technique Partial Least Square Regression (PLSR) capable of reducing the dimensionality of the data with *a priori* knowledge of the classes involved in the analysis: cells that have either been treated with (a) 5FU or (b) paclitaxel. PLS computes a regression of *Y*, a response matrix with dimensions *m×c* where *m* is the number of spectra and *c* is the number of classes, on *X*, an *m×n* spectral data matrix which has *n* number of data points in each spectrum. The *Y* matrix, also known as the design matrix has values of 1 in the column number of the class label, *e.g.* a spectrum belonging to class 2 will have a value of 1 in column 2 the remaining columns are zeros. This technique enabled the visualisation of 2 overlapping populations with a slight offset (Figure 4) demonstrating that, although the analysis of the second derivative spectra revealed almost a superimposition of the features displayed by the action of two different drugs over Caki-2 cells, it is in fact possible to enhance such distinction by analysing the fingerprint region of the IR spectra by means of a chemometric tool, thus opening the possibility of exploring the behaviour of the data as a function of the cell cycle.
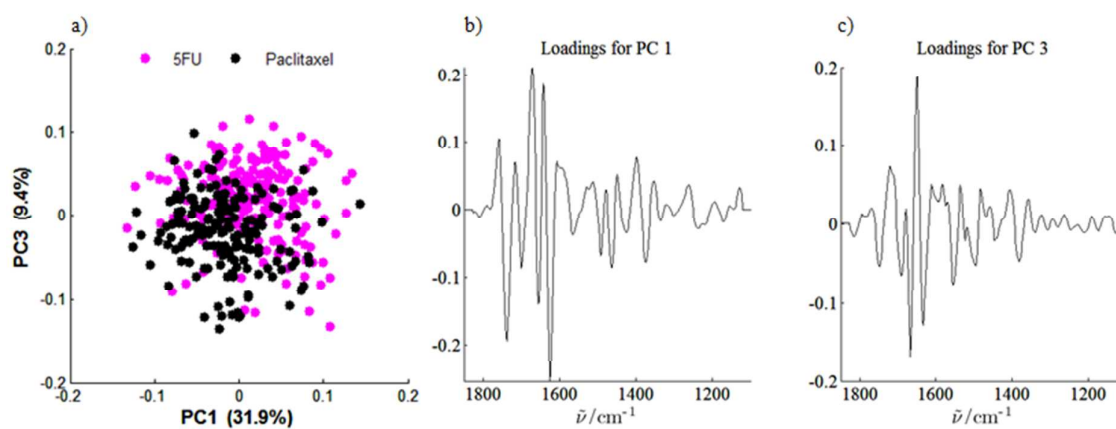
Figure 4. (a) Score plot of RMieS-EMSC corrected data from drug-treated cells over the 1st and 3rd components yielded by PLSR. (b) and (c) are the corresponding loadings along the fingerprint region used for the analysis.

This newly decomposed space is described by the linear combination of the components yielded by the PLS regression of the spectra and therefore it is a synthesized representation of the sources of variability such as drug-treatment and the inherent biochemical changes due to the cell cycle. The left panel in Figure 5 shows the score plot of the FTIR spectra of cells that have been treated with 5FU or paclitaxel as a function of the cell cycle within the exact same space described by Figure 4 a. These images are the result of removing the data points that did not belong to the cell cycle phase of interest.

At first glance it is possible to observe that the cell cycle phases do not cluster within different regions of the scores plot but instead, they tend to overlap each other in order to fully describe the group of data reflecting the treatment to which the cells were exposed: paclitaxel or 5FU. This was the case for the 1st and 3rd components and also for any other pair of coordinates (data nor shown). The behaviour of the data confirms that, by itself, the cell cycle does not account for the major source of variability when the cells are exposed to an anticancer drug[17]. However, this does not mean at all that the inherent biochemical features of the cell cycle can be ignored when trying to give more insight about the mode of action of a particular drug. Thus, in order to demonstrate how each cell cycle phase was affected by the action of these two drugs, the right panel in Figure 5 was created.

The regression of the control spectra, over the space described by the drug-treated data, reveals only biochemical features due to inherent cell cycle. It was computed using the loading vectors that describe drug-treated cells since they contain information regarding (a) cellular response to the drug treatment and (b) cell cycle biochemical features.
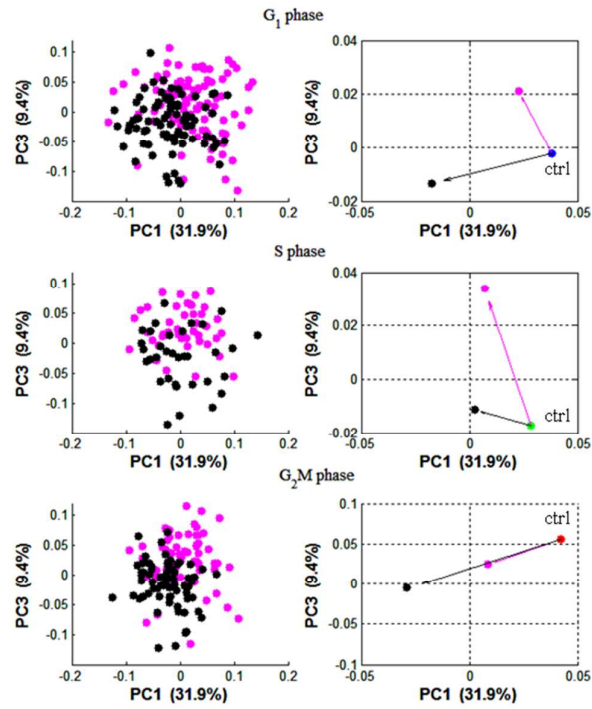
Figure 5. Left panel: Score plot of RMieS-EMSC corrected Caki-2 cells treated with 5FU (pink marks) or Paclitaxel (black marks) described along the 1st and 3rd components of the PLS regression as a function of the cell cycle G_1 (top), S (middle) and G_2M (bottom). Right panel: Centroids of the cell cycle populations from 5FU, Paclitaxel and projection of the Control spectra for G_1 (blue), S (green) and G_2M (red) over the space described by the drug-treated data.

At first glance, it is possible to observe in Figure 5 (right panel) that, among all the cell cycle phases, there is a trend for the spectra of control cells to cluster in the right side of the plot with respect to the drug-treated cells. Despite the 3rd PLS component accounting for 9.4% of the variance of the dataset and enabling the distinction of drug-treated populations along with the 1st component, the coordinate that best describes both treated and control spectra with an overall variance of 31.9% is the 1st component yielded by the PLS regression.

The length of the vector field arrows reflect the global similarity of populations treated with cytotoxics against their control counterparts as they have a common origin. Hence, the shorter the length of the arrow between centroids of the populations described in reduced variance space, the more similar the two populations are in their native spectral characteristics; their clustering trend reveal alike features.

An example of this can be visualized in the score plots corresponding to the S-phase of the cell cycle (see Figure 5 right panel). This figure shows that spectra of paclitaxel-treated cells that were undergoing S-phase at the point of fixation share more spectral features with the control than S-phase cells belonging to the cellular cultures that were exposed to 5FU.

Since treatment with 5FU affects the cells particularly at S-phase of the cell cycle, it is likely that 5FU-treated S-phase cells were being subjected to the action of the drug; causing structural disruption at the nucleic acid level, leading to irreparable cellular damage. Consequently, the extended differences between 5FU-treated S-phase spectra and the S-phase control cells may be due to both (i) the direct effect of the drug on the cells, such as active metabolites being mis-incorporated into the nucleic acids and (ii) the cellular response to treatment.

Conversely, the clustering trend of G_2M phase cells (Figure 5 right panel-bottom) has shown that the greatest difference amongst populations (with the longest vector field arrow), is between the control-G_2M and the paclitaxel-treated G_2M-phase data points. Since treatment with paclitaxel

1
2
3
4
5
6
7
8
9
10
11
12
13
14
15
16
17
18
19
20
21
22
23
24
25
26
27
28
29
30
31
32
33
34
35
36
37
38
39
40
41
42
43
44
45
46
47
48
49
50
51
52
53
54
55
56
57
58
59
60

affects the cells at the G_2M stage of proliferation it is likely that such larger vector field arrow may be indicative of the added variability due to the effect of the drug and the cellular commitment to death due to the apoptotic response triggered by paclitaxel.

This behaviour of the data in a decomposed space, such as PLS, is in agreement with the analysis of the second derivative spectra shown in Figure 2 as paclitaxel-treated spectra of cells undergoing G_2M phase at the point of fixation displayed more pronounced characteristics, particularly in the region from 1420 cm^{-1} to 1020 cm^{-1}, with respect to the control G_2M phase cells.

Conversely, the relatively shorter distance between the centroids of the populations corresponding to the spectra of G_2M-control cells and 5FU-treated G_2M phase cells may indicate that these cells still display spectral characteristics due to the nature of late events of the cell cycle despite their cytotoxic environment.

As proof of principle these results demonstrate that FTIR spectroscopy combined with a supervised chemometric technique such as PLS has the potential to reveal the cell cycle dependent response due to the exposure of a cellular culture to a given anticancer drug. Thus, despite the fact that the cell cycle itself is not the leading clustering trend of an asynchronous culture of cells exposed to any drug, it is only by analysing the data as a function of the cell cycle phases that the mechanism of drug action can be chemically defined.

The drugs used in this study were chosen on the basis of their well-known modes of action and therefore on their capability for disrupting the progression of cells undergoing specific events of the cell cycle: S-phase or G_2M phase due to the action of 5FU or paclitaxel respectively. Furthermore, the fact that G_1-phase cells exposed to any treatment –without the drugs exerting their action on them yet– differ from the control in both of the PLS score plots and also in their native spectral features may be indicative that along with the inherent biochemical processes due to the progression of the

cell through the cell cycle there is also convoluted spectral information regarding the stress at which the cells are exposed in such cytotoxic environment.

The observations yielded by the analysis of the RMieS-EMSC corrected data and the clustering trend of drug-treated spectra against their control counterparts appear to be linked to the mode of action of each drug when taking into consideration the cell cycle dependency. Nevertheless, due to the rich and complex nature of the loadings used to describe the PLS space, the data was subjected to a second pre-processing in order to enable the visualisation of the data in a much simpler configuration, namely *bivariate* space in which the number of variables analysed simultaneously are reduced to two.

The new variables taken into consideration were either the absorbance values at particular wavenumbers or the relative ratios corresponding to the mean absorbance of the peaks centred at (i) 1084 cm^{-1} (nucleic acids), (ii) 1152 cm^{-1} (carbohydrates in the form of glycogen, glycoproteins or sugars), (iii) 1657 cm^{-1} (variations in the protein content revealed by the Amide I band) and (iv) 2852 cm^{-1} and 2958 cm^{-1} (changes in the nature of the acyl chains of lipids).

Among the reasons for which these particular bands have been selected as the variables that will ultimately lead to the definition of the new planes describing the data are, in the first place, the fact that the molecular motions which take place at these wavenumbers represent distinct types of macromolecules within the cells that have shown to vary as a function of both the cell cycle and the cellular treatment, as revealed by the analysis of the second derivative spectra in Figure 2.

Additionally, it has been suggested that the reduction of the protein content of cells that have been treated with drugs may be related to the cleavage of such proteins due to the action of apoptotic caspases, proteosome function or acidification of the cytoplasm due to the stress to which the cells are exposed(*38*). Conversely, it has been demonstrated that apoptosis, being a highly conserved

mechanism among living organisms(*37*), is characterised by a concomitant increase in the methylene

signal arising from the acyl chain in lipids and a considerable reduction of the nucleic acids(*33-36*).

Figure 6 shows the plots yielded by the bivariate analysis of the spectral dataset in which both drug-

treatment and cell cycle dependency are taken into consideration. It is important, however, to point

out that for simplicity and clarity only the centroids of the cell cycle phases within each major

population (control or drug-treated cells) are displayed in the figures.

Figure 6 (a) shows the scatter plot of the absorbance values corresponding to the bands at 1657 cm^{-1}

and 1152 cm^{-1} due to the vibration of proteins and carbohydrates respectively. This figure

demonstrates that spectra of cells exposed to a cytotoxic compound display a consistent increase in

the proportion of carbohydrates while the protein content is reduced. These observations are in

agreement with the overall behaviour of the data in the form of the second derivative spectra

(Figure 2); by analysing the normalised absorbance values at given wavenumbers, *e.g.* Figure 6 (a), it

becomes easier to both visualise and correlate the biochemical changes due to the action of drugs

on a given cell line and also to identify the relative magnitude of change. Thus, the figure in panel (a)

indicates that both drugs induced a similar change in the metabolism of cells. However the

treatment with paclitaxel has promoted the reduction of protein along with the accumulation of

carbohydrates in a more dramatic fashion than the action of 5FU on Caki-2 cells.

Alterations in the metabolism of carbohydrates in cells undergoing apoptosis due to the action of

tyrosine kinase inhibitors (TKIs) such as Imatinib-mesylate and Dasatinib, have been previously

reported by Bellisola *et al.*(*16*) based on their observations of the spectroscopic features of a well-

established mouse model of human Chronic Myelogenous Leukaemia treated with TKIs. The results

presented in Figure 6 (a) demonstrate that a completely different cell line, Caki-2, exposed to the

action of two different anticancer drugs, paclitaxel and 5FU, have not only induced a similar

response, irrespective of the drugs' mode of action, but also that such response seems to be related

to the relatively more efficient induction of apoptosis in Caki-2 cells due to the action of paclitaxel,

as revealed by the quantification of caspase-3 moieties by Zall *et al*.(*39*)
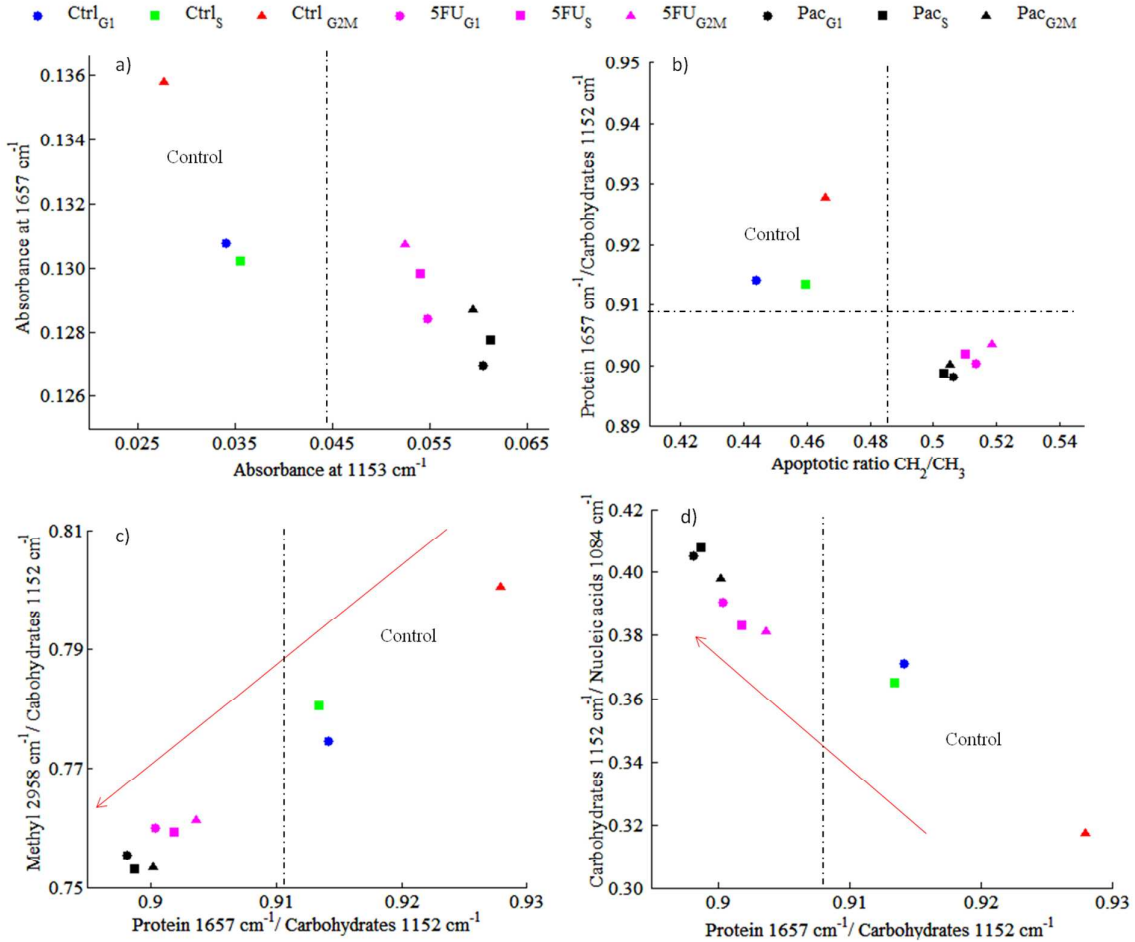
Figure 6. Bivariate analysis of the spectra of Caki-2 cells that have grown under normal culture conditions (control cells in blue, green and red) or exposed to the action of 5FU or Paclitaxel (drug-treated cells in pink or black marks respectively). The cell cycle phases of each population are identified as follows: G1-phase, S-phase and G_2M phase data points are circles,squares and triangles respectively.

It has been demonstrated that the relative content of methylene (CH_2) respect to methyl (CH_3) in

cells varies as a function of both cellular growth(*38*) and progression of apoptosis(*34-36*). It was

therefore necessary to explore the spectral dataset containing data from 3 well-defined cell cycle

phases and information regarding the cellular response to the drug exposure in terms of the

methylene and methyl content. Figure 6 (b) shows the 2-dimensional scatter plot of the ratio

between protein/carbohydrates against the ratio between methylene/methyl. Interestingly, this newly created plane seems to separate the control dataset from the drug treated spectra in both axes, indicating that along with the reduction of protein and increase of carbohydrates content there is also a concomitant increase of methylene moieties, with respect to the methyl groups present in the cells that seems to be dependent upon the cellular response to the treatment. This figure also reveals that, within each population –ctrl, 5FU and paclitaxel–, the largest amount of methylene-based compounds is found in the spectra of cells undergoing later events of the cell cycle such as G_2M phase. These observations are in agreement with previous reports that suggest that such an increase of methylene in late events of the cell cycle is due to the generation of second messengers that regulate cellular growth and which is lipidic in nature (*38*). Variations in the nature of both lipids and proteins, has shown to be more pronounced in cells that were exposed to paclitaxel, as revealed by the red arrow in Figure 6 (c). Similarly, Figure 6 (d) indicates that although both drug treatments have induced variations in the carbohydrates to nucleic acids ratio, paclitaxel-treated cells displayed greater variance in their biochemistry than 5FU-treated cells. Liu *et al.*(*34*) have demonstrated that the amount of detectable DNA in the infrared spectra of cells undergoing apoptosis decreases as a function of the apoptotic index of such cultures and therefore the infrared bands due to the vibration of nucleic acids reveal how committed the cells are into the apoptotic process. Thus, the behaviour of the data in Figure 6 is in agreement with previous publications regarding the induction of apoptosis via different compounds in several fixed cells lines studied by FTIR spectroscopy and also in living models analysed using proton nuclear magnetic resonance. Our results therefore demonstrate that, after 24 hours of exposure, the FTIR spectra of cells exposed to both 5FU and paclitaxel are not only displaying the inherent biochemical fingerprint of cellular growth but also information regarding both the mode of action as a function of the cell cycle and the cellular commitment to death via apoptosis.

The entire spectral dataset was used to build a linear support vector machine (SVM)(*40*) capable of recognizing whether the spectra belonged to (a) the control, (b) 5FU-treated cells or (c) paclitaxel-

treated cells with an average accuracy of 92.7% (see Table 1). Validation of the models was performed via 10-fold cross-validation (see supplementary information). Upon introduction of cell cycle phase information to the algorithm, the classification accuracy dropped to 83.7%; yet, the cell cycle phases were retrieved by the SVM. This indicates that it is possible to determine the cell cycle phases of a culture treated with an anticancer drug by applying supervised and sophisticated algorithms for classifying different populations based on their spectral fingerprint.

Table 1. Prediction accuracy for the SVM constructed to identify drug-treatment and cell cycle phase of Caki-2 cells

Population	Classification accuracy, %
Control	98
5FU	89
Paclitaxel	91
Cell cycle phase of untreated (control) and drug-treated cells.	**Classification accuracy, %**
$G_0 - G_1$	80
S	82
$G_2 - M$	89

Conclusion

FTIR micro-spectroscopy coupled with multivariable and bivariate analytical techniques has been shown to yield straightforward valuable information regarding the stage at which Caki-2 cells were affected by the action of 5FU and paclitaxel. Furthermore, the cell cycle phases of this renal cell line were shown to be retrieved successfully by means of an optimized linear support vector machine. Although this investigation supports the fact that the biochemical features due to the proliferation itself are not the leading clustering trend of cells exposed to an anticancer drug, our study highlights the need to take into consideration the spectral fingerprint of the underlying cell cycle when analysing anticancer agents *in –vitro*, particularly when such agents' mode of action remains to be elucidated or when the agents are known to disrupt the cell cycle at a given stage of proliferation.

Caspase 3 staining clearly demonstrated that 24h exposure to IC_{50} concentration of these cytotoxic agents was sufficient to initiate apoptosis. The cellular response to either 5FU or paclitaxel was

consistently overimposed by the prominent spectral features of apoptosis *i.e.* change in the nature of the lipids and reduction of protein content. In this context, further investigation at shorter exposure times with multiple drugs is required in order to reliably assign spectral patterns to particular modes of action.

References

1. Cancer multidrug resistance, *Nat Biotech*.
2. Nussbaumer, S., Bonnabry, P., Veuthey, J. L., and Fleury-Souverain, S. (2011) Analysis of anticancer drugs: a review, *Talanta 85*, 2265-2289.
3. Scharovsky, O. G., Mainetti, L. E., and Rozados, V. R. (2009) Metronomic chemotherapy: changing the paradigm that more is better, *Curr Oncol 16*, 7-15.
4. Derenne, A., Gasper, R., and Goormaghtigh, E. (2011) The FTIR spectrum of prostate cancer cells allows the classification of anticancer drugs according to their mode of action, *The Analyst 136*, 1134.
5. Derenne, A., Verdonck, M., and Goormaghtigh, E. (2012) The effect of anticancer drugs on seven cell lines monitored by FTIR spectroscopy, *Analyst 137*, 3255-3264.
6. Hughes, C., Brown, M. D., Clarke, N. W., Flower, K. R., and Gardner, P. (2012) Investigating cellular responses to novel chemotherapeutics in renal cell carcinoma using SR-FTIR spectroscopy, *Analyst 137*, 4720-4726.
7. Hughes, C., Brown, M. D., Ball, F. J., Monjardez, G., Clarke, N. W., Flower, K. R., and Gardner, P. (2012) Highlighting a need to distinguish cell cycle signatures from cellular responses to chemotherapeutics in SR-FTIR spectroscopy, *Analyst 137*, 5736-5742.
8. Draux, F., Jeannesson, P., Gobinet, C., Sule-Suso, J., Pijanka, J., Sandt, C., Dumas, P., Manfait, M., and Sockalingum, G. D. (2009) IR spectroscopy reveals effect of non-cytotoxic doses of anti-tumour drug on cancer cells, *Analytical and Bioanalytical Chemistry 395*, 2293-2301.
9. Gasper, R., Dewelle, J., Kiss, R., Mijatovic, T., and Goormaghtigh, E. (2009) IR spectroscopy as a new tool for evidencing antitumor drug signatures, *Biochimica et Biophysica Acta (BBA) - Biomembranes 1788*, 1263-1270.
10. Gasper, R., Mijatovic, T., Bénard, A., Derenne, A., Kiss, R., and Goormaghtigh, E. (2010) FTIR spectral signature of the effect of cardiotonic steroids with antitumoral properties on a prostate cancer cell line, *Biochimica et Biophysica Acta (BBA) - Molecular Basis of Disease 1802*, 1087-1094.
11. Gasper, R., Mijatovic, T., Kiss, R., and Goormaghtigh, E. (2010) FTIR spectroscopy reveals the concentration dependence of cellular modifications induced by anticancer drugs, *Spectroscopy 24*, 45-49.
12. Gasper, R., Vandenbussche, G., and Goormaghtigh, E. (2011) Ouabain-induced modifications of prostate cancer cell lipidome investigated with mass spectrometry and FTIR spectroscopy, *Biochimica et Biophysica Acta (BBA) - Biomembranes 1808*, 597-605.
13. Berger, G., Gasper, R., Lamoral-Theys, D., Wellner, A., Gelbcke, M., Gust, R., Neve, J., Kiss, R., Goormaghtigh, E., and Dufrasne, F. (2010) Fourier transform infrared (FTIR) spectroscopy to monitor the cellular impact of newly synthesized platinum derivatives, *Int J Oncol 37*, 679-686.
14. Flower, K. R., Khalifa, I., Bassan, P., Demoulin, D., Jackson, E., Lockyer, N. P., McGown, A. T., Miles, P., Vaccari, L., and Gardner, P. (2011) Synchrotron FTIR analysis of drug treated ovarian A2780 cells: an ability to differentiate cell response to different drugs?, *Analyst 136*, 498-507.
15. Bellisola, G., Della Peruta, M., Vezzalini, M., Moratti, E., Vaccari, L., Birarda, G., Piccinini, M., Cinque, G., and Sorio, C. (2010) Tracking InfraRed signatures of drugs in cancer cells by Fourier Transform microspectroscopy, *The Analyst 135*, 3077.
16. Bellisola, G., Cinque, G., Vezzalini, M., Moratti, E., Silvestri, G., Redaelli, S., Gambacorti Passerini, C., Wehbe, K., and Sorio, C. (2013) Rapid recognition of drug-resistance/sensitivity in leukemic cells by Fourier transform infrared microspectroscopy and unsupervised hierarchical cluster analysis, *Analyst 138*, 3934-3945.

17. Derenne, A., Mignolet, A., and Goormaghtigh, E. (2013) FTIR spectral signature of anticancer drug effects on PC-3 cancer cells: is there any influence of the cell cycle?, *Analyst 138*, 3998-4005.

18. Sulé-Suso, J., Skingsley, D., Sockalingum, G. D., Kohler, A., Kegelaer, G., Manfait, M., and El Haj, A. J. (2005) FT-IR microspectroscopy as a tool to assess lung cancer cells response to chemotherapy, *Vibrational Spectroscopy 38*, 179-184.

19. Jamin, N., Miller, L., Moncuit, J., Fridman, W. H., Dumas, P., and Teillaud, J. L. (2003) Chemical heterogeneity in cell death: combined synchrotron IR and fluorescence microscopy studies of single apoptotic and necrotic cells, *Biopolymers 72*, 366-373.

20. Meade, A. D., Clarke, C., Byrne, H. J., and Lyng, F. M. (2010) Fourier transform infrared microspectroscopy and multivariate methods for radiobiological dosimetry, *Radiat Res 173*, 225-237.

21. Longley, D. B., Harkin, D. P., and Johnston, P. G. (2003) 5-Fluorouracil: mechanisms of action and clinical strategies, *Nature Reviews Cancer 3*, 330-338.

22. Rowinsky, E. K. (1993) Clinical pharmacology of Taxol, *J Natl Cancer Inst Monogr*, 25-37.

23. Vichai, V., and Kirtikara, K. (2006) Sulforhodamine B colorimetric assay for cytotoxicity screening, *Nature Protocols 1*, 1112-1116.

24. Gazi, E., Dwyer, J., Lockyer, N. P., Miyan, J., Gardner, P., Hart, C., Brown, M., and Clarke, N. W. (2005) Fixation protocols for subcellular imaging by synchrotron-based Fourier transform infrared microspectroscopy, *Biopolymers 77*, 18-30.

25. Clemens, G., Flower, K. R., Henderson, A. P., Whiting, A., Przyborski, S. A., Jimenez-Hernandez, M., Ball, F., Bassan, P., Cinque, G., and Gardner, P. (2013) The action of all-trans-retinoic acid (ATRA) and synthetic retinoid analogues (EC19 and EC23) on human pluripotent stem cells differentiation investigated using single cell infrared microspectroscopy, *Mol Biosyst 9*, 677-692.

26. Jimenez-Hernandez, M., Hughes, C., Bassan, P., Ball, F., Brown, M. D., Clarke, N. W., and Gardner, P. (2013) Exploring the spectroscopic differences of Caki-2 cells progressing through the cell cycle while proliferating in vitro, *Analyst 138*, 3957-3966.

27. Bassan, P., Kohler, A., Martens, H., Lee, J., Byrne, H. J., Dumas, P., Gazi, E., Brown, M., Clarke, N., and Gardner, P. (2010) Resonant Mie scattering (RMieS) correction of infrared spectra from highly scattering biological samples, *Analyst 135*, 268-277.

28. Bassan, P., Kohler, A., Martens, H., Lee, J., Jackson, E., Lockyer, N., Dumas, P., Brown, M., Clarke, N., and Gardner, P. (2010) RMieS-EMSC correction for infrared spectra of biological cells: Extension using full Mie theory and GPU computing, *Journal of Biophotonics 3*, 609-620.

29. Savitzky, A., and Golay, M. J. E. (1964) Smoothing and Differentiation of Data by Simplified Least Squares Procedures, *Analytical Chemistry 36*, 1627-1639.

30. Mark, H., and Workman Jr, J. (2007) 75 - The Chemometrics of Imaging Spectroscopy, In *Chemometrics in Spectroscopy*, pp 503-XXI, Academic Press, Amsterdam.

31. Movasaghi, Z., Rehman, S., and ur Rehman, D. I. (2008) Fourier Transform Infrared (FTIR) Spectroscopy of Biological Tissues, *Applied Spectroscopy Reviews 43*, 134-179.

32. Diem M, G. P., Chalmers J. M. (2008) *Vibrational spectroscopy for medical diagnosis*, 1 ed., Wiley, Boston, US.

33. Gaudenzi, S., Pozzi, D., Toro, P., Silvestri, I., Morrone, S., and Castellano, A. C. (2004) Cell apoptosis specific marker found by Fourier Transform Infrared Spectroscopy, *Spectroscopy-an International Journal 18*, 415-422.

34. Liu, K. Z., Jia, L., Kelsey, S. M., Newland, A. C., and Mantsch, H. H. (2001) Quantitative determination of apoptosis on leukemia cells by infrared spectroscopy, *Apoptosis 6*, 269-278.

35. Blankenberg, F. G., Katsikis, P. D., Storrs, R. W., Beaulieu, C., Spielman, D., Chen, J. Y., Naumovski, L., and Tait, J. F. (1997) Quantitative analysis of apoptotic cell death using proton nuclear magnetic resonance spectroscopy, *Blood 89*, 3778-3786.
36. Zhang, G. Y., Zhu, R. Y., Xu, Y., Yan, Y. B., and Dai, Y. R. (2004) Increase in methylene resonance signal intensity is associated with apoptosis in plant cells as detected by H-1-NMR, *Acta Botanica Sinica 46*, 711-718.
37. Elmore, S. (2007) Apoptosis: A Review of Programmed Cell Death, *Toxicologic Pathology 35*, 495-516.
38. Gasparri, F., and Muzio, M. (2003) Monitoring of apoptosis of HL60 cells by Fourier-transform infrared spectroscopy, *Biochem J 369*, 239-248.
39. Zall, H., Weber, A., Besch, R., Zantl, N., and Hacker, G. (2010) Chemotherapeutic drugs sensitize human renal cell carcinoma cells to ABT-737 by a mechanism involving the Noxa-dependent inactivation of Mcl-1 or A1, *Molecular Cancer 9*, 164.
40. Chang, C.-C., and Lin, C.-J. (2011) LIBSVM: A library for support vector machines, *ACM Trans. Intell. Syst. Technol. 2*, 1-27.